

Tripartite entanglement in $H \rightarrow ZZ, WW$ decays

J. A. Aguilar-Saavedra

Instituto de Física Teórica IFT-UAM/CSIC, c/Nicolás Cabrera 13–15, 28049 Madrid, Spain

Abstract

The decays of the Higgs boson produce a state in which the spins of the decay products and the orbital angular momentum (L) are highly entangled. We obtain the tripartite density operator, as well as reduced operators, for the decay into two weak bosons. For $H \rightarrow ZZ$ in the four-lepton final state we also estimate the statistical sensitivity at the Large Hadron Collider and future upgrades, using a binned method to reconstruct the density operators from distributions. With the expected Run 3 data, establishing genuine tripartite entanglement would be possible beyond the 5σ level. The violation of Bell inequalities involving the spins of the two weak bosons could also be established beyond the 5σ level.

1 Introduction

High-energy physics experiments offer a new playground to test quantum entanglement at the energy frontier, with proposals to test the spin entanglement of pairs of top quarks [1–8], muons [9], τ leptons [10], weak bosons [11–17], as well as particles of different spin [18–20]. It is well known that, in addition to spin, particle production and decay involves orbital angular momentum (hereafter referred to as L). Therefore, in the aforementioned examples not only the spins of the two particles S_1, S_2 may be entangled, but they can also be entangled with L , as a consequence of total angular momentum conservation. An obvious step further is then to test the tripartite entanglement between S_1, S_2 and L in these processes. The Hilbert space for L , in which the eigenstates $|lm\rangle$, with $l = 0, \dots, \infty$ and $m = -l, \dots, l$ form an orthonormal basis, has infinite dimension in general. However, in decay processes the conservation of total angular momentum implies that only a finite-dimensional subspace \mathcal{H}_L is relevant. For example, in Higgs boson decays to weak boson pairs VV , $V = W, Z$, we have $l \leq 2$, and \mathcal{H}_L is 9-dimensional. Likewise, in $H \rightarrow \tau^+\tau^-$, \mathcal{H}_L has dimension four, with $l \leq 1$.

The Higgs boson is the only elementary scalar, and its decays produce highly-entangled states. In this work we address the tripartite entanglement in $H \rightarrow VV$ decays, working in the Hilbert space $\mathcal{H}_L \otimes \mathcal{H}_{S_1} \otimes \mathcal{H}_{S_2}$. We use the method proposed in Ref. [21] to determine density operators involving L . In contrast to spin, the density operators involving L cannot be directly measured from angular distributions. But they can be related, in a model-independent fashion, to measurable quantities. This is done by exploiting the complementarity between:

- (i) Helicity amplitudes [22], in which the spin of the parent particle is quantised in some fixed axis \hat{z} , but for the decay products it is quantised in their direction of motion. These

amplitudes depend on a small set of parameters that in principle can be measured in data.

- (ii) Canonical amplitudes, in which the spin of all particles is quantised in a fixed direction \hat{z} . These amplitudes allow to build the multi-partite density operators involving L and the spins of the decay products.

The relation between these sets is model-independent, and arises from a simple change of basis for the spinors and polarisation vectors entering the amplitudes. It has been used in Ref. [21] to write down the full density operator for top quark decays $t \rightarrow Wb$, which involves L as well as the spins of the W boson and b quark. For $H \rightarrow VV$, the helicity amplitudes depend on three complex quantities. Once these quantities are measured in data, the full 81-dimensional density operator for L and the spins of the two weak bosons can be determined. It turns out that L , S_1 and S_2 are genuinely entangled, that is, no bipartition of the (LS_1S_2) system is separable. Tracing over L degrees of freedom, one obtains the density operator for the two spin degrees of freedom S_1 and S_2 , which are highly entangled. Tracing over one of the spins S_i , $i = 1, 2$, the density operator for LS_j ($j \neq i$) is found. We provide leading-order calculations for all these density operators in the Standard Model (SM) as well as methods to determine them from experimental data. We also provide estimates of the statistical sensitivity to establish the entanglement between the different parties in $H \rightarrow ZZ \rightarrow 4\ell$, with $\ell = e, \mu$, at the Large Hadron Collider (LHC) and its future high-luminosity upgrade (HL-LHC).

2 Higgs decay amplitudes

Let us consider a general two-body decay of a spin- J particle with third spin component M , described in a coordinate system with a basis $\{\hat{x}, \hat{y}, \hat{z}\}$ in its rest frame. In the helicity framework of Jacob and Wick [22] the decay amplitudes have the general form

$$A_{M\lambda_1\lambda_2}^h(\theta, \phi) = a_{\lambda_1\lambda_2} D_{M\lambda}^{J*}(\phi, \theta, 0), \quad (1)$$

where λ_1 and λ_2 are the helicities of the decay products, $\lambda = \lambda_1 - \lambda_2$, $a_{\lambda_1\lambda_2}$ are independent of the angles and $D_{m'm}^j(\alpha, \beta, \gamma)$ are the Wigner functions

$$D_{mm'}^j \equiv \langle jm' | e^{-i\alpha J_3} e^{-i\beta J_2} e^{-i\gamma J_3} | jm \rangle. \quad (2)$$

The angles (θ, ϕ) correspond to the first decay product (with helicity λ_1). In the case of a scalar decay, $D_{00}^0 = 1$, and therefore the helicities are equal. Furthermore, for a scalar decay into vector bosons, the helicity amplitudes are parameterised by three quantities a_{11} , a_{00} , a_{-1-1} . The same parameters enter the canonical amplitudes. For an on-shell decay, these parameters are constant; however, for $H \rightarrow VV$, they depend on the invariant mass of the off-shell V boson m_{V^*} , or equivalently, on the modulus of the three-momenta in the Higgs rest frame, which we denote as q .

The canonical amplitudes $A_{s_1 s_2}^c$ (we omit the trivial index M) are found by changing the basis for the polarisation vectors. For a vector boson with momentum

$$p_V = (E_V, q \sin \theta \cos \phi, q \sin \theta \sin \phi, q \cos \theta) \quad (3)$$

the polarisation vectors in the helicity basis are

$$\begin{aligned} \varepsilon_h^{(+)} &= -\frac{1}{\sqrt{2}}(0, \cos \theta \cos \phi - i \sin \phi, \cos \theta \sin \phi + i \cos \phi, -\sin \theta), \\ \varepsilon_h^{(0)} &= \frac{1}{M_V}(q, E_V \sin \theta \cos \phi, E_V \sin \theta \sin \phi, E_V \cos \theta), \\ \varepsilon_h^{(-)} &= \frac{1}{\sqrt{2}}(0, \cos \theta \cos \phi + i \sin \phi, \cos \theta \sin \phi - i \cos \phi, -\sin \theta). \end{aligned} \quad (4)$$

On the other hand, the polarisation vectors in the fixed basis are

$$\begin{aligned} \varepsilon_R^{(+)} &= \varepsilon_R^{(+)} - \frac{1}{\sqrt{2}} \sin \theta e^{i\phi} \frac{q}{M_V} \left(1, \frac{\vec{p}}{M_V + E_V} \right), \\ \varepsilon_R^{(0)} &= \varepsilon_R^{(0)} + \cos \theta \frac{q}{M_W} \left(1, \frac{\vec{p}}{M_V + E_V} \right), \\ \varepsilon_R^{(-)} &= \varepsilon_R^{(-)} + \frac{1}{\sqrt{2}} \sin \theta e^{-i\phi} \frac{q}{M_V} \left(1, \frac{\vec{p}}{M_V + E_V} \right), \end{aligned} \quad (5)$$

where

$$\begin{aligned} \varepsilon_R^{(+)} &= -\frac{1}{\sqrt{2}}(0, 1, i, 0), \\ \varepsilon_R^{(0)} &= (0, 0, 0, 1), \\ \varepsilon_R^{(-)} &= \frac{1}{\sqrt{2}}(0, 1, -i, 0) \end{aligned} \quad (6)$$

are the V rest-frame polarisation vectors. With this change of basis, the canonical amplitudes acquire a dependence on (θ, ϕ) that is not present in the helicity amplitudes for a scalar decay. Expanding them in terms of spherical harmonics Y_l^m , and bearing in mind that $\langle \Omega | lm \rangle = Y_l^m(\Omega)$, with $\Omega = (\theta, \phi)$, one can identify the amplitudes into L eigenstates $A_{s_1 s_2; lm}$.

The non-zero ones are

$$\begin{aligned} A_{11;2-2} &= A_{-1-1;22} = -\sqrt{\frac{2\pi}{15}}(a_{11} + 2a_{00} + a_{-1-1}), \\ A_{10;2-1} &= A_{01;2-1} = A_{0-1;21} = A_{-10;21} = \sqrt{\frac{\pi}{15}}(a_{11} + 2a_{00} + a_{-1-1}), \\ A_{1-1;20} &= A_{-11;20} = -\sqrt{\frac{2\pi}{45}}(a_{11} + 2a_{00} + a_{-1-1}), \\ A_{00;20} &= -\sqrt{\frac{4\pi}{45}}(a_{11} + 2a_{00} + a_{-1-1}), \\ A_{10;1-1} &= -A_{1-1;10} = -A_{01;1-1} = A_{0-1;11} = A_{-11;10} = -A_{-10;11} = \sqrt{\frac{\pi}{3}}(a_{11} - a_{-1-1}), \\ A_{1-1;00} &= -A_{00;00} = A_{-11;00} = -\sqrt{\frac{4\pi}{9}}(a_{11} - a_{00} + a_{-1-1}). \end{aligned} \quad (7)$$

We finally note that, for an off-shell vector boson as in $H \rightarrow VV$, the propagator includes a scalar degree of freedom. Here we will be interested in decays into light charged leptons $\ell = e, \mu$ and neutrinos, and when coupled to massless external fermions the scalar component vanishes [23]; therefore, we can safely consider the off-shell W as a spin-1 particle. This assumption is supported by the comparison of analytical and Monte Carlo calculations.

3 Density operators for Higgs decay

Angular momentum in the two-body decay $H \rightarrow VV$ is described by a density operator $\rho_{LS_1S_2}$ acting on the Hilbert space $\mathcal{H}_L \otimes \mathcal{H}_{S_1} \otimes \mathcal{H}_{S_2}$. For fixed m_{V^*} (or q), it can be calculated from the decay amplitudes found in the previous section as

$$(\rho_{LS_1S_2})_{s_1s_2;lm}^{s'_1s'_2;l'm'} = A_{s_1s_2;lm} A_{s'_1s'_2;l'm'}^*. \quad (8)$$

Notice that $\rho_{LS_1S_2}$ as calculated from this equation always corresponds to a pure state. As mentioned, a_{11} , a_{00} , a_{-1-1} depend on m_{V^*} . The kinematical distribution of this quantity, calculated with MADGRAPH [26] at the leading order, is presented in Fig. 1 for $H \rightarrow WW$ and $H \rightarrow ZZ$. In practice, Eq. (8) can be used to calculate the density operator within some interval of m_{V^*} . For example, in $H \rightarrow ZZ$ with $m_{Z^*} \in [18, 32]$ GeV (which amounts to 55% of the events) the exact density operator calculated with Monte Carlo describes a pure state up to corrections of the order of 0.5%. Likewise, for $H \rightarrow WW$ with $m_{W^*} \in [30, 44]$ GeV (49% of the events) the density operator corresponds to a pure state up to corrections of 1%. Therefore, using (8) is quite a good approximation even for bin widths of the order of 10 GeV.

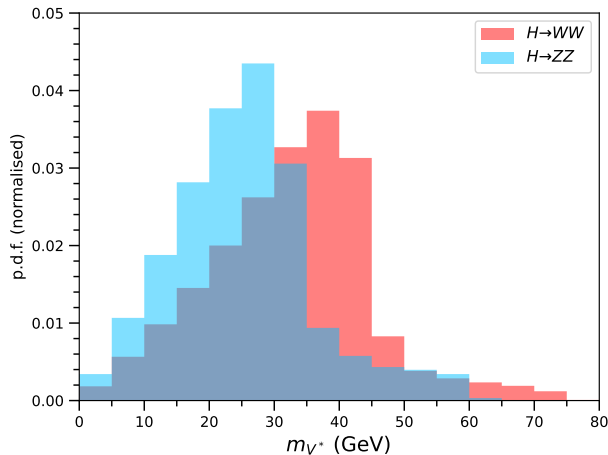


Figure 1: Invariant mass distribution of the off-shell boson in Higgs decays to WW and ZZ .

In order to obtain $\rho_{LS_1S_2}$ for the full decay phase space we use Monte Carlo calculations of $gg \rightarrow H \rightarrow ZZ \rightarrow e^+e^-\mu^+\mu^-$ and $gg \rightarrow H \rightarrow W^+W^- \rightarrow \ell^+\nu\ell^-\nu$ with MADGRAPH, using 7×10^6 and 10^7 events, respectively. In $H \rightarrow ZZ$, we label the boson with largest

invariant mass as V_1 , and in $H \rightarrow W^+W^-$ we select $V_1 = W^+$. (In any case, the predictions are symmetric under interchange $1 \leftrightarrow 2$.) We divide the m_{V^*} range in 2 GeV intervals and, within each bin ‘ k ’, the values of a_{11} , a_{00} and a_{-1-1} are extracted from Monte Carlo pseudo-data (see section 5 for details) using parton-level information.¹ The density operator $\rho_{LS_1S_2}^{(k)}$ for that bin is calculated using (8), and the theoretical prediction for $\rho_{LS_1S_2}$ in the full m_{V^*} range is obtained by summing the operators $\rho_{LS_1S_2}^{(k)}$ in the different bins, with the appropriate weight. This density operator no longer describes a pure state, but it is quite close. For $H \rightarrow ZZ$, the principal eigenvector has eigenvalue 0.966 (where unity would correspond to a pure state), and in $H \rightarrow WW$ the principal eigenvector has eigenvalue 0.963.

Tracing over the Hilbert space of any of the subsystems \mathcal{H}_L , \mathcal{H}_{S_1} , or \mathcal{H}_{S_2} , we obtain the reduced density operators for the other two, respectively $\rho_{S_1S_2}$, ρ_{LS_2} , and ρ_{LS_1} . These operators correspond to the marginalisation over the corresponding degree of freedom. Tracing over two of the subsystems one obtains the density operator for a single subsystem. For the spin degrees of freedom, and since the scalar decay does not have any preferred direction, the operators describe a completely unpolarised state,

$$\rho_{S_1} = \rho_{S_2} = \frac{1}{3} \begin{pmatrix} 1 & 0 & 0 \\ 0 & 1 & 0 \\ 0 & 0 & 1 \end{pmatrix}, \quad (9)$$

by construction. For L , the density operator is diagonal, and for fixed m_{V^*} it has entries

$$\begin{aligned} (\rho_L)_{2m}^{2m} &= \frac{1}{30} \frac{1}{\mathcal{N}} |a_{11} + 2a_{00} + a_{-1-1}|^2, \\ (\rho_L)_{1m}^{1m} &= \frac{1}{6} \frac{1}{\mathcal{N}} |a_{11} - a_{-1-1}|^2, \\ (\rho_L)_{00}^{00} &= \frac{1}{3} \frac{1}{\mathcal{N}} |a_{11} - a_{00} + a_{-1-1}|^2, \end{aligned} \quad (10)$$

with

$$\mathcal{N} = |a_{11}|^2 + |a_{00}|^2 + |a_{-1-1}|^2. \quad (11)$$

For the full phase space, the Monte Carlo calculation yields $(\rho_L)_{2m}^{2m} = 0.021$, $(\rho_L)_{1m}^{1m} = 0$, $(\rho_L)_{00}^{00} = 0.895$ for both $H \rightarrow ZZ$ and $H \rightarrow WW$. It is worthwhile pointing out that, even if the Higgs decay is isotropic, there are $l = 2$ contributions (as well as $l = 1$ contributions if CP is broken in the decay). Note that

$$\sum_{m=-2}^2 |Y_2^m(\theta, \phi)|^2 = \frac{5}{4\pi}, \quad \sum_{m=-1}^1 |Y_1^m(\theta, \phi)|^2 = \frac{3}{4\pi}. \quad (12)$$

This cancellation of the angular dependence makes apparent the need to determine ρ_L indirectly from the measurement of a_{11} , a_{00} and a_{-1-1} , because one cannot directly access it through distributions [21].

¹As a cross-check, we do the same in 5 GeV intervals. The numerical results are the same, with differences in the range $10^{-4} - 10^{-3}$.

The entanglement between one of the subsystems (L , S_1 or S_2) and the rest can be tested by taking the partial transpose of $\rho_{LS_1S_2}$ over the corresponding space \mathcal{H}_L , \mathcal{H}_{S_1} , or \mathcal{H}_{S_2} . For a bipartite system AB (such as \mathcal{H}_L versus $\mathcal{H}_{S_1} \otimes \mathcal{H}_{S_2}$) the entanglement can be characterised by the Peres-Horodecki [27,28] criterion. Since the positivity of the partial transpose over any subsystem, say ρ^{TB} , is a necessary condition for separability, a non-positive ρ^{TB} is a sufficient condition for entanglement. Furthermore, the amount of entanglement can be quantified by the negativity of ρ^{TB} [29],

$$N(\rho) = \frac{\|\rho^{TB}\| - 1}{2}, \quad (13)$$

where $\|X\| = \text{tr} \sqrt{XX^\dagger} = \sum_i \sqrt{\lambda_i}$, where λ_i are the (positive) eigenvalues of the matrix XX^\dagger . Equivalently, $N(\rho)$ equals the sum of the negative eigenvalues of ρ^{TB} . (The result is the same when taking the partial transpose on subsystem A .) In the separable case $N(\rho) = 0$. For pure states the generalised concurrence [30] can also be used as entanglement measure. For a bipartite system AB , it is defined as

$$C^2 = 2(1 - \text{tr} \rho_A^2), \quad (14)$$

with ρ_A the reduced density operator obtained by trace over the B degrees of freedom. The result is the same when tracing over \mathcal{H}_A , and in the separable case $C^2 = 0$.

These tests, performed for the three possible bipartitions, give sufficient conditions for genuine tripartite entanglement, that is, that the state is not separable under any bipartition of $\mathcal{H}_L \otimes \mathcal{H}_{S_1} \otimes \mathcal{H}_{S_2}$. The entanglement measures between the different bipartitions are collected in Table 1, for the full decay phase space as well as on selected bins of m_{V^*} , in which the Higgs decay produces a pure state to an excellent approximation.²

	$L-(S_1S_2)$	$S_1-(LS_2)$	$S_2-(LS_1)$
$H \rightarrow ZZ$ inclusive	$N = 0.757$	$N = 0.998$	$N = 0.998$
$H \rightarrow ZZ$, $m_{Z^*} \in [25, 30]$ GeV	$N = 0.421$ $C^2 = 0.108$	$N = 1$ $C^2 = 4/3$	$N = 1$ $C^2 = 4/3$
$H \rightarrow WW$ inclusive	$N = 0.746$	$N = 0.998$	$N = 0.998$
$H \rightarrow WW$, $m_{W^*} \in [35, 40]$ GeV	$N = 0.376$ $C^2 = 0.088$	$N = 1$ $C^2 = 4/3$	$N = 1$ $C^2 = 4/3$

Table 1: Entanglement measures for the different bipartitions of $\mathcal{H}_L \otimes \mathcal{H}_{S_1} \otimes \mathcal{H}_{S_2}$.

For pure states the entanglement between one spin S_i and the rest of the system is maximal. This is easily understood because the Higgs decay is isotropic: tracing over the (LS_j) subsystem ($j \neq i$) yields the reduced operator (9), which corresponds to an unpolarised state. Consequently, for the $S_i-(LS_j)$ entanglement the concurrence C^2 takes its maximal value

²A global measure of the tripartite entanglement for unequal systems of these dimensions ($9 \times 3 \times 3$) is not currently available in the literature.

for systems of the dimensionality $(9 \times 3 \times 3)$ under consideration. The tripartite operators transposed in the spaces \mathcal{H}_{S_1} or \mathcal{H}_{S_2} have three eigenvalues $-1/3$, so that for S_i -(LS_j) entanglement one has $N = 1$. Both $C^2 = 4/3$ and $N = 1$ are guaranteed by construction when one writes the $\rho_{LS_1S_2}$ operator from Eq. (8). For the full phase space, in which $\rho_{LS_1S_2}$ is a weighted sum of pure states $\rho_{LS_1S_2}^{(k)}$, N is still quite close to unity. A similar property does not hold for L -(S_1S_2) entanglement. As it follows from Eqs. (12) and the related discussion, there are many (infinite) possibilities for ρ_L consistent with a Higgs isotropic decay.

One can also investigate the entanglement between a pair of subsystems, when the third one is marginalised. The eigenvalue λ_{\max} of the principal eigenvector is also of interest, in order to assess to which extent the reduced density operators correspond to a pure state. Both are presented in Table 2. The L - S_i subsystems are weakly entangled, and in a very mixed state with $\lambda_{\max} \leq 1/3$. This is in agreement with the fact that the entanglement between one spin and the rest of the system is maximal, as discussed above. On the other hand, the entanglement between the two spins is quite large, and their state, even after tracing over L degrees of freedom, is relatively close to a pure state.

	L - S_1	L - S_2	S_1 - S_2
$H \rightarrow ZZ$ inclusive	$\lambda_{\max} = 0.322$ $N = 0.105$	$\lambda_{\max} = 0.322$ $N = 0.105$	$\lambda_{\max} = 0.896$ $N = 0.843$
$H \rightarrow ZZ, M_{Z^*} \in [25, 30]$ GeV	$\lambda_{\max} = 1/3$ $N = 0.038$	$\lambda_{\max} = 1/3$ $N = 0.038$	$\lambda_{\max} = 0.972$ $N = 0.959$
$H \rightarrow WW$ inclusive	$\lambda_{\max} = 0.321$ $N = 0.102$	$\lambda_{\max} = 0.321$ $N = 0.102$	$\lambda_{\max} = 0.895$ $N = 0.843$
$H \rightarrow WW, M_{W^*} \in [35, 40]$ GeV	$\lambda_{\max} = 1/3$ $N = 0.031$	$\lambda_{\max} = 1/3$ $N = 0.031$	$\lambda_{\max} = 0.977$ $N = 0.966$

Table 2: Eigenvalue of the principal eigenvector and negativity for the different pairs of systems when the third one is traced out.

4 Spin entanglement and Bell inequalities

The spin entanglement between the two weak bosons has already been addressed for $H \rightarrow WW$ [11, 13–16] and $H \rightarrow ZZ$ [12, 15, 16] in the helicity basis $\{\hat{r}, \hat{n}, \hat{k}\}$ where the quantisation axis \hat{k} is taken in the flight direction of V_1 , $\hat{k} = (\theta, \phi)$. The density operator is obtained after integration over all decay phase space with this ‘moving’ coordinate system. The angular integration is trivial in this case because the Higgs decay is isotropic. On the other hand, the operator $\rho_{S_1S_2}$ obtained in the previous section parameterises the spin state of the VV pair with a fixed basis $\{\hat{x}, \hat{y}, \hat{z}\}$ and integrated over all decay phase space — the angular integration is not trivial in this case because we fix a preferred direction. Both descriptions

are not equivalent. In the former case, for $H \rightarrow ZZ$ (and similarly for $H \rightarrow WW$) the density operator has an eigenvector

$$|\psi\rangle = 0.444 [|1-1\rangle_{\hat{k}} + |-11\rangle_{\hat{k}}] - 0.777 |00\rangle_{\hat{k}}, \quad (15)$$

with eigenvalue 0.970. In the latter, the density operator has as principal eigenvector the spin singlet

$$|\psi\rangle = \frac{1}{\sqrt{3}} [|1-1\rangle - |00\rangle + |-11\rangle] \quad (16)$$

with eigenvalue 0.896. The numerical value of the entanglement measure N is quite similar in both cases, however.

In this section we address spin entanglement and possible violation of Bell inequalities using the reduced density operator in the canonical basis as obtained in the previous section. We parameterise $\rho_{S_1 S_2}$ in terms of irreducible tensor operators T_m^l , with $l = 1, 2$ and $-l \leq m \leq l$, acting on the three-dimensional spin space for each boson [12]. For convenience we normalise T_m^l such that $\text{tr} [T_m^l (T_m^l)^\dagger] = 3$, where $(T_m^l)^\dagger = (-1)^m T_{-m}^l$. Specifically, the operators are defined as

$$\begin{aligned} T_{\pm 1}^1 &= \mp \frac{\sqrt{3}}{2} (J_1 \pm iJ_2), & T_0^1 &= \sqrt{\frac{3}{2}} J_3, \\ T_{\pm 2}^2 &= \frac{2}{\sqrt{3}} (T_{\pm 1}^1)^2, & T_{\pm 1}^2 &= \sqrt{\frac{2}{3}} [T_{\pm 1}^1 T_0^1 + T_0^1 T_{\pm 1}^1], \\ T_0^2 &= \frac{\sqrt{2}}{3} [T_1^1 T_{-1}^1 + T_{-1}^1 T_1^1 + 2(T_0^1)^2], \end{aligned} \quad (17)$$

with J_i the usual spin operators in the Cartesian basis. In terms of these, the spin density operator reads [12]

$$\rho_{S_1 S_2} = \frac{1}{9} \left[\mathbb{1}_3 \otimes \mathbb{1}_3 + A_{lm}^1 T_m^l \otimes \mathbb{1}_3 + A_{lm}^2 \mathbb{1}_3 \otimes T_m^l + C_{l_1 m_1 l_2 m_2} T_{m_1}^{l_1} \otimes T_{m_2}^{l_2} \right], \quad (18)$$

with a sum over all indices. The coefficients satisfy the relations

$$\begin{aligned} (A_{lm}^{1,2})^* &= (-1)^m A_{l-m}^{1,2}, \\ (C_{l_1 m_1 l_2 m_2})^* &= (-1)^{m_1+m_2} C_{l_1 -m_1 l_2 -m_2}. \end{aligned} \quad (19)$$

For fixed m_{V^*} , it is found that the only non-zero coefficients are³

$$\begin{aligned} C_{1010} &= -C_{111-1} = -C_{1-111} \equiv C_1, \\ C_{2020} &= C_{222-2} = C_{2-222} = -C_{212-1} = -C_{2-121} \equiv C_2, \end{aligned} \quad (20)$$

with

$$\begin{aligned} C_1 &= \frac{1}{2} \frac{1}{\mathcal{N}} \{ -|a_{11}|^2 - |a_{-1-1}|^2 + 2 \text{Re} [(a_{11} + a_{-1-1}) a_{00}^*] \}, \\ C_2 &= \frac{1}{2} \frac{1}{\mathcal{N}} \{ |a_{11}|^2 + 4|a_{00}|^2 + |a_{-1-1}|^2 - 6 \text{Re} [(a_{11} + a_{-1-1}) a_{00}^*] \\ &\quad + 12 \text{Re} [a_{11} a_{-1-1}^*] \}. \end{aligned} \quad (21)$$

³These relations different from (and not to be confused with) the ones found for the helicity basis [13].

For the full decay phase space the relations (21) with helicity amplitudes do not hold, but the relations between coefficients (20) still do because the density operator depends linearly on them. Therefore, the full phase-space reduced operator $\rho_{S_1 S_2}$ can be written as the expansion (18) in terms of two independent coefficients C_1 and C_2 . The eigenvalues of the partial transpose $\rho_{S_1 S_2}^{T_B}$ are

$$\begin{aligned}\lambda_5 &= \frac{1}{18}(2 - 3C_1 + C_2) \quad (\text{quintuple}), \\ \lambda_3 &= \frac{1}{18}(2 + 3C_1 - 5C_2) \quad (\text{triple}), \\ \lambda_1 &= \frac{1}{9}(2 + 3C_1 + 5C_2).\end{aligned}\tag{22}$$

By the Peres-Horodecki criterion, finding any of these eigenvalues negative is a sufficient condition for spin entanglement. Given the SM values $C_1 = -0.844$, $C_2 = 0.906$ (both for ZZ and WW), only λ_3 is expected to be negative, $\lambda_3 = -0.281$, and a useful entanglement test that is equivalent to the negativity, $N = -3\lambda_3$.

Concerning Bell-like inequalities, for a Hilbert space $\mathcal{H}_A \otimes \mathcal{H}_B$ with both subsystems A, B having dimension 3, a powerful test is provided by the Collins-Gisin-Linden-Massar-Popescu (CGLMP) inequality [31]: for observables A_1, A_2 in \mathcal{H}_A , and observables B_1, B_2 in \mathcal{H}_B , we have

$$\begin{aligned}I_3 &= P(A_1 = B_1) + P(B_1 = A_2 + 1) + P(A_2 = B_2) + P(B_2 = A_1) - P(A_1 = B_1 - 1) \\ &\quad - P(B_1 = A_2) - P(A_2 = B_2 - 1) - P(B_2 = A_1 - 1) \leq 2\end{aligned}\tag{23}$$

in any local realistic theory. Here, $P(B_i = A_j + a)$ is the probability that the measurements of B_i gives the same result as the measurement of A_j plus a , modulo 3. This inequality can be conveniently written in terms of Bell operators $\mathcal{O}_{\text{Bell}}$, such that

$$I_3 \equiv \langle \mathcal{O}_{\text{Bell}} \rangle = \text{tr}[\mathcal{O}_{\text{Bell}} \rho_{S_1 S_2}] \leq 2\tag{24}$$

in a local realistic theory. A choice of Bell operator that is optimal for the maximally-entangled spin-singlet state is [32]

$$\mathcal{O}_{\text{Bell}} = \frac{4}{3\sqrt{3}}(T_1^1 \otimes T_{-1}^1 + T_{-1}^1 \otimes T_1^1) + \frac{2}{3}(T_2^2 \otimes T_{-2}^2 + T_{-2}^2 \otimes T_2^2).\tag{25}$$

However, the VV pair is not produced in a pure spin-singlet state. An operator that gives a larger value for I_3 in the helicity basis was found in Ref. [12],

$$\begin{aligned}\mathcal{O}'_{\text{Bell}} &= -\frac{4}{3\sqrt{3}}T_0^1 \otimes T_0^1 + \frac{1}{2}T_0^2 \otimes T_0^2 + \frac{2}{3\sqrt{3}}(T_1^1 \otimes T_{-1}^1 + T_{-1}^1 \otimes T_1^1) \\ &\quad - \frac{1}{3}(T_1^2 \otimes T_{-1}^2 + T_{-1}^2 \otimes T_1^2) + \frac{1}{12}(T_2^2 \otimes T_{-2}^2 + T_{-2}^2 \otimes T_2^2).\end{aligned}\tag{26}$$

In the canonical basis, and given the relations (20) between coefficients, both operators are equivalent. We compare in Table 3 the values obtained for I_3 in the helicity basis (as used in previous works) and in the canonical basis, using both operators.

	$H \rightarrow ZZ$		$H \rightarrow WW$	
	$\mathcal{O}_{\text{Bell}}$	$\mathcal{O}'_{\text{Bell}}$	$\mathcal{O}_{\text{Bell}}$	$\mathcal{O}'_{\text{Bell}}$
Helicity	2.327	2.691	2.270	2.629
Canonical	2.507		2.506	

Table 3: Values of the quantity I_3 signaling violation of the CGLMP inequalities.

5 Parameter determination

A model-independent measurement of a_{11} , a_{00} and a_{-1-1} and their relative phases is possible from angular distributions. For the decay $V_1 V_2 \rightarrow f_1 f'_1 f_2 f'_2$ we label as $(\theta_{1,2}, \phi_{1,2})$ the polar and azimuthal angles of $f_{1,2}$ in the $V_{1,2}$ rest frame, with respect to some coordinate system to be specified later. Then, corresponding to a density operator of the form (18), the four-dimensional angular distribution is [12, 13]

$$\frac{1}{\sigma} \frac{d\sigma}{d\Omega_1 d\Omega_2} = \frac{1}{(4\pi)^2} \left[1 + A_{lm}^1 B_l Y_l^m(\theta_1, \phi_1) + A_{lm}^2 B_l Y_l^m(\theta_2, \phi_2) + C_{l_1 m_1 l_2 m_2} B_{l_1} B_{l_2} Y_{l_1}^{m_1}(\theta_1, \phi_1) Y_{l_2}^{m_2}(\theta_2, \phi_2) \right], \quad (27)$$

with B_1, B_2 constants. For $H \rightarrow ZZ$, and taking $f_{1,2}$ as the negative leptons, one has

$$B_1 = -\sqrt{2\pi}\eta_\ell, \quad B_2 = \sqrt{\frac{2\pi}{5}} \quad (28)$$

with

$$\eta_\ell = \frac{1 - 4s_W^2}{1 - 4s_W^2 + 8s_W^4} \simeq 0.13, \quad (29)$$

s_W being the sine of the weak mixing angle. For $H \rightarrow WW$, $B_{1,2}$ are as in (28) setting $\eta_\ell = 1$ for ℓ^- and $\eta_\ell = -1$ for ℓ^+ .

As we have remarked in the introduction, the extraction of the parameters a_{11} , a_{00} and a_{-1-1} from data (or pseudo-data) is done by using the helicity basis $\{\hat{r}, \hat{n}, \hat{k}\}$, defined as follows:

- The \hat{k} axis is taken in the direction of the V_1 three-momentum in the Higgs boson rest frame.
- The \hat{r} axis is in the production plane and defined as $\hat{r} = \text{sign}(\cos\theta)(\hat{p}_p - \cos\theta\hat{k})/\sin\theta$, with $\hat{p}_p = (0, 0, 1)$ the direction of one proton in the laboratory frame, $\cos\theta = \hat{k} \cdot \hat{p}_p$. The definition for \hat{r} is the same if we use the direction of the other proton $-\hat{p}_p$.
- The \hat{n} axis is taken such that $\hat{n} = \hat{k} \times \hat{r}$, orthogonal to the production plane.

This reference system is used to measure the angles $(\theta_{1,2}, \phi_{1,2})$. Implicitly, this requires the reconstruction of the rest frames of the decaying bosons. This is straightforward for

$H \rightarrow ZZ \rightarrow 4\ell$, whereas for $H \rightarrow WW \rightarrow \ell\nu\ell\nu$ the system is underconstrained and the kinematics cannot be uniquely determined. Promising attempts have been made in this direction using machine-learning techniques [24]. Alternatively, one can consider the semi-leptonic decay mode $H \rightarrow WW \rightarrow \ell\nu q\bar{q}'$ [14], in which the full reconstruction is possible and the discrimination between jets originating from up- and down-type quarks is achieved with charm tagging.

In the remainder of this section we show how the parameters a_{11} , a_{00} , a_{-1-1} can be extracted from data. We will present a model-independent extraction, followed by a method that assumes CP conservation in the $H \rightarrow VV$ decay.

5.1 Model-independent parameter determination

In the helicity basis, and considering fixed m_{V^*} , the non-zero coefficients in the expansion (18) are given by [13]⁴

$$\begin{aligned}
A_{20}^1 &= A_{20}^2 = \frac{1}{\sqrt{2}} \frac{1}{\mathcal{N}} [|a_{11}|^2 + |a_{-1-1}|^2 - 2|a_{00}|^2] , \\
C_{1010} &= -\frac{3}{2} \frac{1}{\mathcal{N}} [|a_{11}|^2 + |a_{-1-1}|^2] , \\
C_{2020} &= \frac{1}{2} \frac{1}{\mathcal{N}} [|a_{11}|^2 + |a_{-1-1}|^2 + 4|a_{00}|^2] , \\
C_{222-2} &= C_{2-222}^* = 3 \frac{1}{\mathcal{N}} a_{11} a_{-1-1}^* , \\
C_{111-1} &= -C_{212-1} = C_{1-111}^* = -C_{2-121}^* = -\frac{3}{2} \frac{1}{\mathcal{N}} [a_{11} a_{00}^* + a_{00} a_{-1-1}^*]
\end{aligned} \tag{30}$$

and, when CP is broken,

$$\begin{aligned}
A_{10}^1 &= -A_{10}^2 = \sqrt{\frac{3}{2}} \frac{1}{\mathcal{N}} [|a_{11}|^2 - |a_{-1-1}|^2] , \\
C_{1020} &= -C_{2010} = \frac{\sqrt{3}}{2} \frac{1}{\mathcal{N}} [|a_{11}|^2 - |a_{-1-1}|^2] , \\
C_{1-121} &= -C_{2-111} = C_{112-1}^* = -C_{211-1}^* = \frac{3}{2} \frac{1}{\mathcal{N}} [a_{00} a_{11}^* - a_{-1-1} a_{00}^*] .
\end{aligned} \tag{31}$$

In the following we set $\mathcal{N} = 1$ for simplicity, as the global normalisation is irrelevant. By using the relation $|a_{11}|^2 + |a_{00}|^2 + |a_{-1-1}|^2 = 1$, one can combine the measurements of A_{20}^1 and A_{20}^2 to find $|a_{00}|$, and the measurements of A_{10}^1 and A_{10}^2 to determine $|a_{11}|$ and $|a_{-1-1}|$. Alternatively, one can use the $\cos\theta_{1,2}$ distributions. By integrating Eq. (27) and using the above relations, one obtains

$$\begin{aligned}
\frac{1}{\sigma} \frac{d\sigma}{d\cos\theta_1} &= \frac{3}{8} |a_{11}|^2 (1 - 2\eta_\ell \cos\theta_1 + \cos^2\theta_1) + \frac{3}{4} |a_{00}|^2 \sin^2\theta_1 \\
&\quad + \frac{3}{8} |a_{-1-1}|^2 (1 + 2\eta_\ell \cos\theta_1 + \cos^2\theta_1) ,
\end{aligned} \tag{32}$$

⁴These relations are different from (and not to be confused with) the ones presented for the canonical basis in section 4.

and likewise for θ_2 . For W boson decays this distribution is well known [33]. A fit to the distribution with the constraint $|a_{11}|^2 + |a_{00}|^2 + |a_{-1-1}|^2 = 1$ provides the three moduli. Again, the distributions for θ_1 and θ_2 can be used to improve the determination. The relative phase between a_{11} and a_{-1-1} is found from the measurement of C_{222-2} . The relative phase between a_{11} and a_{00} can be obtained by measuring for example C_{212-1} and C_{2-111} .

5.2 Determination in the CP-conserving case

Within the SM, CP is conserved in $H \rightarrow VV$ decays at the leading order (LO), and $a_{11} = a_{-1-1}$. CP-violating effects in the SM arise beyond the LO but are at the level of 10^{-5} [25]. Therefore, CP conservation is quite a mild assumption that greatly reduces the statistical uncertainty in the determination of the amplitudes. Because $a_{11} = a_{-1-1}$, the moduli of the three parameters can be determined from either measurements of A_{20}^1 or A_{20}^2 , and the two statistically-independent measurements can be combined. The relative sign between a_{11} and a_{00} is fixed by the Lorentz structure of the vertex [12].

6 Sensitivity in $H \rightarrow ZZ$

In this section we assess the statistical uncertainty in the measurement of various entanglement observables in $pp \rightarrow H \rightarrow ZZ \rightarrow 4\ell$ the LHC, using Run 2 + Run 3 data, and at the HL-LHC. For the calculation of the expected number of events we use state-of-the-art values of the Higgs production cross section and branching ratio into four electrons or muons. The cross section at next-to-next-to-next-to-leading order is 48.61 pb, 52.23 pb and 54.67 pb at centre-of-mass energies of 13, 13.6 and 14 TeV [34], and the Higgs branching ratio decay into four leptons (electrons or muons) is 1.24×10^{-4} [34]. The assumed luminosities are 350 fb $^{-1}$ for Runs 2+3 and 3 ab $^{-1}$ for HL-LHC. In order to have a more realistic estimate of the number of events in each case a lepton detection efficiency of 0.7 is assumed, yielding an overall detection efficiency of 0.25. This efficiency accounts for the minimum transverse momentum (p_T) thresholds required for lepton detection. We do not include any trigger requirement. The presence of four leptons from the Higgs decay, some of them with significant p_T , is expected to fulfill one or many of the trigger conditions for one, two, or three leptons [35]. In addition, we include the efficiency of the invariant mass cut required to remove the interference in same-flavour final states (see the appendix). Overall, the expected number of events for Runs 2+3 and HL-LHC are $N = 490$ and $N = 4500$, respectively.

We do not include backgrounds in our analysis. The $H \rightarrow ZZ \rightarrow 4\ell$ signal is quite clean, and its main background is the electroweak process $pp \rightarrow ZZ/Z\gamma \rightarrow 4\ell$, which is about 4 times smaller at the Higgs peak [36]. Although a background subtraction is necessary to obtain the relevant signal distributions, the main effect of the presence of this small background is a slight increase in the statistical uncertainty of the measurement.

	theory	Runs 2+3	HL-LHC
$\rho_{LS_1}, \lambda_{\max}$	0.966	0.970	0.976
$\rho_{LS_{1,2}}, \lambda_{\max}$	0.322	0.323	0.325
$\rho_{S_1S_2}, \lambda_{\max}$	0.896	0.897	0.905

Table 4: Theoretical predictions for the eigenvalues of the principal eigenvectors, and central values obtained from pseudo-experiments.

	theory	Runs 2+3	HL-LHC
$L-(S_1S_2), N$	0.757	0.75 ± 0.14	5.3σ $0.75 \pm 0.05 \gg 5\sigma$
$S_i-(LS_j), N$	0.998	1.0 ± 0.004	$\gg 5\sigma$ $0.998 \pm 0.001 \gg 5\sigma$
$L-S_{1,2}, N$	0.105	$0.106 \pm 0.032^*$	4.3σ $0.102 \pm 0.010 \gg 5\sigma$
S_1-S_2, N	0.843	$0.85 \pm 0.05^*$	$\gg 5\sigma$ $0.857 \pm 0.014 \gg 5\sigma$
$S_1-S_2, \mathcal{O}_{\text{Bell}}$	2.507	$2.51 \pm 0.11^*$	3.8σ $2.539 \pm 0.033 \gg 5\sigma$
$S_1-S_2, \mathcal{O}'_{\text{Bell}}$ (helicity)	2.691	$2.65 \pm 0.09^*$	5.7σ $2.678 \pm 0.035 \gg 5\sigma$

Table 5: Theoretical predictions of several entanglement observables, and their central values and statistical uncertainties obtained from pseudo-experiments. For those marked with an asterisk, the p.d.f. is not Gaussian but skew-normal (see the text). The statistical significance for $N > 0$, or $I_3 > 2$, is also included.

The statistical uncertainty is estimated by performing pseudo-experiments. In each pseudo-experiment, a subset of N random events is drawn from the total event set, and for this subset the density operators are calculated as discussed in section 3, using the parameter determination in the CP-conserving case. Because the number of events is not large, we use three m_{V^*} bins of 20 GeV. From the density operators, the eigenvalues of the principal eigenvectors, the entanglement measures N , and I_3 , signalling violation of the Bell inequalities are obtained. A large number of 2×10^4 pseudo-experiments is performed in order to obtain the probability density function (p.d.f.) of these quantities. The coarse binning used is sufficient even for the statistics of the HL-LHC, as it can be checked by comparing the central values obtained from the pseudo-experiments with those previously obtained in section 3. A first test is provided by the eigenvalues of the principal eigenvectors. These are collected in Table 4. As it can be readily observed, the agreement is excellent.

The central values and statistical uncertainties for the entanglement observables of interest are presented in Table 5, together with their theoretical prediction from section 3.⁵ Again, the agreement between the central values and the theoretical calculations using the full event sample and 2 GeV bins is very good, and sufficient for the statistical uncertainties present. The p.d.f.'s for entanglement observables are shown in Figs. 2 and 3. We omit those for

⁵For $\mathcal{O}'_{\text{Bell}}$ in the helicity basis the same binned method of section 3 is employed, but using instead Eqs. (30) for the determination of the density operator.

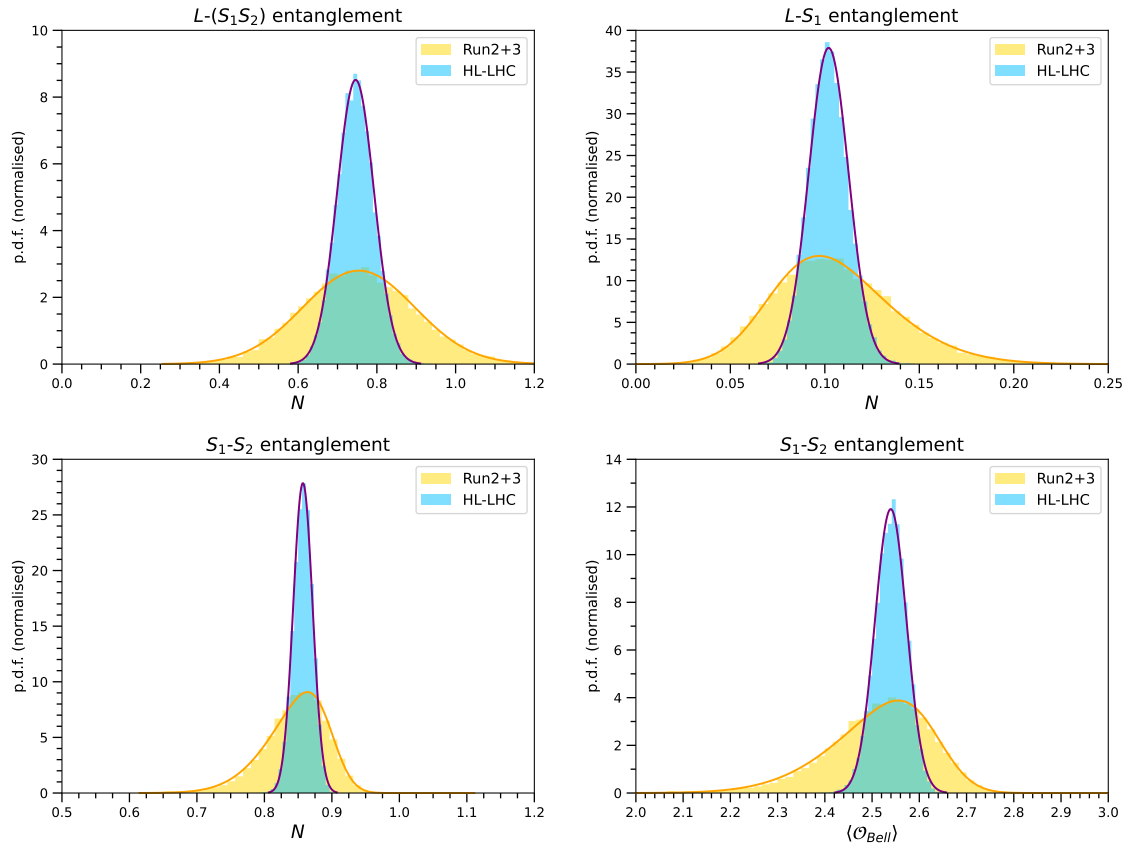


Figure 2: Probability density functions for entanglement observables in the canonical basis, as obtained from the pseudo-experiments. The solid lines represent the best-fit Gaussian or skew-normal distributions.

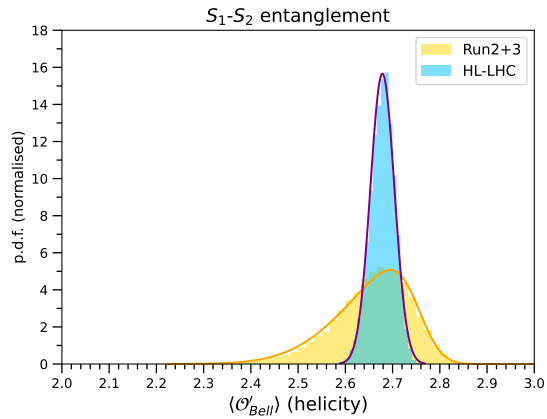


Figure 3: Probability density functions for $\langle \mathcal{O}'_{Bell} \rangle$ in the helicity basis, as obtained from the pseudo-experiments. The solid lines represent the best-fit Gaussian or skew-normal distributions.

S_i -(LS_j) and L - S_2 entanglement; for the former, all the pseudo-experiments give values in an extremely narrow range, and the latter is similar to L - S_1 . For several observables, marked with an asterisk in Table 5, the p.d.f. is not Gaussian for the small number of events expected in LHC Runs 2+3. Still, the p.d.f. is very well approximated by a skew-normal distribution. In those cases, the statistical significances are computed by using the skew-normal distribution with the parameters that best fit the numerical p.d.f. resulting the pseudo-experiments. The statistical significances for entanglement, $N > 0$, and violation of Bell inequalities, $I_3 > 2$, are also presented in Table 5.

The improvement of statistical uncertainties achieved with this binned reconstruction method is remarkable. If systematic uncertainties are under control, it allows to establish genuine tripartite entanglement in $H \rightarrow ZZ$ decays beyond the 5σ level at the current LHC run. Also, it allows to verify the violation of Bell inequalities between the two boson spins beyond the 5σ level.

7 Discussion

This work extends previous entanglement studies in $H \rightarrow VV$ in two aspects. First, we have generalised the framework to include L , thereby being able to study its entanglement with the weak boson spins. Second, we have devised a method to improve the statistical precision in the determination of density operators from data. This method, necessary to obtain the tripartite density operator involving L , involves binning the m_{V^*} distribution and using theoretical input to obtain the density operator $\rho_{LS_1S_2}^{(k)}$ for each bin, from measurements of robust observables. The density operator $\rho_{LS_1S_2}$ for the full decay phase space is then obtained with a weighted sum of the different bin contributions. This determination is especially resilient against statistical fluctuations in data when CP conservation is assumed in the decay. Notably, it can also be used to improve the extraction of S_1S_2 operators in the helicity basis, considered in previous work.

While we have focused on the density operators integrated on the full m_{V^*} range for simplicity, experimental measurements in bins are possible provided there are sufficient statistics. A potential problem for our approach would be event migration between bins, but we expect the impact of this effect in our results to be limited, due to the great similarity between the predictions obtained for 20 GeV bins and 2 GeV bins.

We have not addressed detailed sensitivity estimations for $H \rightarrow WW$. Still, a few remarks are in place. In the semi-leptonic channel $WW \rightarrow \ell\nu q\bar{q}'$, Ref. [14] used charm tagging to identify the jet corresponding to an initial down-type quark, to be used as spin analyser. Within our framework, where we reconstruct the density operator from measurements of A_{20} , the quark identification is not necessary because $Y_2^0(\theta, \phi) = Y_2^0(\pi - \theta, \phi + \pi)$. Similarly, the yet unexplored decay channel $H \rightarrow ZZ \rightarrow \ell^+\ell^-q\bar{q}$ offers good prospects for experimental measurements.

Finally, our estimation of the expected statistical uncertainties for $H \rightarrow ZZ \rightarrow 4\ell$ offers excellent prospects, improving over previous results for S_1 - S_2 entanglement [12] that also assumed CP conservation in the decay. For most entanglement observables considered, including violation of Bell inequalities in the $S_1 S_2$ system, a statistical significance over 5σ is expected for the combination of LHC Run 2 and Run 3 data, and for all observables the statistical significance is way above the 5σ level at HL-LHC.

Acknowledgements

This work has been supported by the Spanish Research Agency (Agencia Estatal de Investigación) through projects PID2019-110058GB-C21, PID2022-142545NB-C21 and CEX2020-001007-S funded by MCIN/AEI/10.13039/501100011033, and by Fundação para a Ciência e a Tecnologia (FCT, Portugal) through the project CERN/FIS-PAR/0019/2021.

A Identical particles in $H \rightarrow ZZ$ decay

The decays $H \rightarrow ZZ \rightarrow 4e$ and $H \rightarrow ZZ \rightarrow 4\mu$ involve identical particles in the final state, and two contributing diagrams where they are interchanged. While one cannot properly speak about which Z boson decayed to which opposite-sign pair, because of the interference between diagrams, by a suitable invariant mass selection one can reduce that interference to negligible levels.

We test the effect of identical-particle exchange by generating a sample of $pp \rightarrow H \rightarrow 4e$ with 7.8×10^6 events. There are two possible pairings of opposite-sign leptons, ‘a’ and ‘b’, and for each combination we have two invariant masses $m_{e_1^+ e_1^-}$, $m_{e_2^+ e_2^-}$. We select the pairing that produces an opposite-sign pair with the maximum invariant mass, namely the maximum among $m_{e_1^+ e_1^-}^{(a)}$, $m_{e_2^+ e_2^-}^{(a)}$, $m_{e_1^+ e_1^-}^{(b)}$, $m_{e_2^+ e_2^-}^{(b)}$. Once the lepton pairing is selected, we identify V_1 as the Z boson decaying into the highest invariant mass pair, and measure angular distributions as described in section 5. We apply the selection $m_{V_1} \geq 80$ GeV to reduce the interference effects. This cut has an efficiency of 0.77.

The effect in angular distributions of identical-particle exchange can be assessed by comparing the values of non-zero coefficients in the four-dimensional distribution (27), for the $H \rightarrow ZZ \rightarrow e^+ e^- \mu^+ \mu^-$ and the $H \rightarrow ZZ \rightarrow 4e$ samples. We collect them in the left panel of Table 6. In addition, one can compare the principal eigenvalues λ_{\max} of the different density operators, extracted from data using the model-independent method outlined in section 5, and entanglement measures N between different subsystems. We collect them in the right panel of Table 6. It turns out that the differences have not practical importance even for the higher statistics collected at the HL-LHC.

	$e^+e^-\mu^+\mu^-$	$4e$		$e^+e^-\mu^+\mu^-$	$4e$
$B_2A_{20}^1$	-0.636	-0.639	$\rho_{LS_1S_2}, \lambda_{\max}$	0.966	0.961
$B_2A_{20}^2$	-0.634	-0.640	$\rho_{LS_i}, \lambda_{\max}$	0.322	0.321
$B_1^2C_{111-1}$	0.10	0.21	$\rho_{S_1S_2}, \lambda_{\max}$	0.896	0.890
$B_1^2C_{1010}$	-0.067	-0.11	$S_i-(LS_j), N$	0.998	1.0
$B_2^2C_{222-2}$	0.76	0.72	$L-(S_1S_2), N$	0.757	0.776
$B_2^2C_{212-1}$	-1.20	-1.16	$L-S_i, N$	0.105	0.108
$B_2^2C_{2020}$	1.76	1.71	S_1-S_2, N	0.843	0.835

Table 6: Comparison of different quantities between the decays $H \rightarrow ZZ \rightarrow e^+e^-\mu^+\mu^-$ and $H \rightarrow ZZ \rightarrow 4e$ (see the text).

References

- [1] Y. Afik and J. R. M. de Nova, “Entanglement and quantum tomography with top quarks at the LHC,” *Eur. Phys. J. Plus* **136**, no.9, 907 (2021) [arXiv:2003.02280 [quant-ph]].
- [2] M. Fabbrihesi, R. Floreanini and G. Panizzo, “Testing Bell Inequalities at the LHC with Top-Quark Pairs,” *Phys. Rev. Lett.* **127** (2021) no.16, 16 [arXiv:2102.11883 [hep-ph]].
- [3] C. Severi, C. D. Boschi, F. Maltoni and M. Sioli, “Quantum tops at the LHC: from entanglement to Bell inequalities,” *Eur. Phys. J. C* **82**, no.4, 285 (2022) [arXiv:2110.10112 [hep-ph]].
- [4] Y. Afik and J. R. M. de Nova, “Quantum information with top quarks in QCD,” *Quantum* **6**, 820 (2022) [arXiv:2203.05582 [quant-ph]].
- [5] J. A. Aguilar-Saavedra and J. A. Casas, “Improved tests of entanglement and Bell inequalities with LHC tops,” *Eur. Phys. J. C* **82**, no.8, 666 (2022) [arXiv:2205.00542 [hep-ph]].
- [6] Y. Afik and J. R. M. de Nova, “Quantum Discord and Steering in Top Quarks at the LHC,” *Phys. Rev. Lett.* **130**, no.22, 221801 (2023) [arXiv:2209.03969 [quant-ph]].
- [7] Z. Dong, D. Gonçalves, K. Kong and A. Navarro, “When the Machine Chimes the Bell: Entanglement and Bell Inequalities with Boosted $t\bar{t}$,” [arXiv:2305.07075 [hep-ph]].
- [8] T. Han, M. Low and T. A. Wu, “Quantum Entanglement and Bell Inequality Violation in Semi-Leptonic Top Decays,” [arXiv:2310.17696 [hep-ph]].
- [9] J. A. Aguilar-Saavedra, “Decay of entangled fermion pairs with post-selection,” *Phys. Lett. B* **848**, 138409 (2024) [arXiv:2308.07412 [hep-ph]].
- [10] M. M. Altakach, P. Lamba, F. Maltoni, K. Mawatari and K. Sakurai, “Quantum information and CP measurement in $H \rightarrow \tau + \tau^-$ at future lepton colliders,” *Phys. Rev. D* **107**, no.9, 093002 (2023) [arXiv:2211.10513 [hep-ph]].

- [11] A. J. Barr, “Testing Bell inequalities in Higgs boson decays,” *Phys. Lett. B* **825**, 136866 (2022) [arXiv:2106.01377 [hep-ph]].
- [12] J. A. Aguilar-Saavedra, A. Bernal, J. A. Casas and J. M. Moreno, “Testing entanglement and Bell inequalities in $H \rightarrow ZZ$,” *Phys. Rev. D* **107**, no.1, 016012 (2023) [arXiv:2209.13441 [hep-ph]].
- [13] J. A. Aguilar-Saavedra, “Laboratory-frame tests of quantum entanglement in $H \rightarrow WW$,” *Phys. Rev. D* **107**, no.7, 076016 (2023) [arXiv:2209.14033 [hep-ph]].
- [14] F. Fabbri, J. Howarth and T. Maurin, “Isolating semi-leptonic $H \rightarrow WW^*$ decays for Bell inequality tests,” *Eur. Phys. J. C* **84**, no.1, 20 (2024) [arXiv:2307.13783 [hep-ph]].
- [15] R. Ashby-Pickering, A. J. Barr and A. Wierchucka, “Quantum state tomography, entanglement detection and Bell violation prospects in weak decays of massive particles,” *JHEP* **05**, 020 (2023) [arXiv:2209.13990 [quant-ph]].
- [16] M. Fabbrichesi, R. Floreanini, E. Gabrielli and L. Marzola, “Bell inequalities and quantum entanglement in weak gauge bosons production at the LHC and future colliders,” [arXiv:2302.00683 [hep-ph]].
- [17] R. A. Morales, “Exploring Bell inequalities and quantum entanglement in vector boson scattering,” [arXiv:2306.17247 [hep-ph]].
- [18] J. A. Aguilar-Saavedra, “Postdecay quantum entanglement in top pair production,” *Phys. Rev. D* **108**, no.7, 076025 (2023) [arXiv:2307.06991 [hep-ph]].
- [19] J. A. Aguilar-Saavedra and J. A. Casas, “Entanglement autodistillation from particle decays,” [arXiv:2401.06854 [hep-ph]].
- [20] J. A. Aguilar-Saavedra, “A closer look at post-decay $t\bar{t}$ entanglement,” [arXiv:2401.10988 [hep-ph]].
- [21] J. A. Aguilar-Saavedra, “Full quantum tomography of top quark decays,” [arXiv:2402.14725 [hep-ph]].
- [22] M. Jacob and G. C. Wick, “On the General Theory of Collisions for Particles with Spin,” *Annals Phys.* **7**, 404-428 (1959)
- [23] S. Berge, S. Groote, J. G. Körner and L. Kaldamäe, “Lepton-mass effects in the decays $H \rightarrow ZZ^* \rightarrow \ell^+\ell^-\tau^+\tau^-$ and $H \rightarrow WW^* \rightarrow \ell\nu\tau\nu_\tau$,” *Phys. Rev. D* **92**, no.3, 033001 (2015) [arXiv:1505.06568 [hep-ph]].
- [24] M. Grossi, J. Novak, B. Kersevan and D. Rebutzi, “Comparing traditional and deep-learning techniques of kinematic reconstruction for polarization discrimination in vector boson scattering,” *Eur. Phys. J. C* **80**, no.12, 1144 (2020) [arXiv:2008.05316 [hep-ph]].

- [25] A. V. Gritsan, H. Bahl, R. K. Barman, I. Bozovic-Jelisavcic, J. Davis, W. Dekens, Y. Gao, D. Goncalves, L. S. M. Guerra and D. Jeans, *et al.* [arXiv:2205.07715 [hep-ex]].
- [26] J. Alwall, R. Frederix, S. Frixione, V. Hirschi, F. Maltoni, O. Mattelaer, H. S. Shao, T. Stelzer, P. Torrielli and M. Zaro, “The automated computation of tree-level and next-to-leading order differential cross sections, and their matching to parton shower simulations,” JHEP **07**, 079 (2014) [arXiv:1405.0301 [hep-ph]].
- [27] A. Peres, “Separability criterion for density matrices,” Phys. Rev. Lett. **77**, 1413-1415 (1996) [arXiv:quant-ph/9604005 [quant-ph]].
- [28] P. Horodecki, “Separability criterion and inseparable mixed states with positive partial transposition,” Phys. Lett. A **232**, 333 (1997) [arXiv:quant-ph/9703004 [quant-ph]].
- [29] M. B. Plenio and S. Virmani, “An introduction to entanglement measures,” Quant. Inf. Comput. **7**, no.1-2, 001-051 (2007) [arXiv:quant-ph/0504163 [quant-ph]].
- [30] P. Rungta, V. Bužek, C.M. Caves, M. Hillery and G. J. Milburn, “Universal state inversion and concurrence in arbitrary dimensions” Phys. Rev. A **64** no. 4, 042315 (2001) [arXiv:quant-ph/0102040]
- [31] D. Collins, N. Gisin, N. Linden, S. Massar and S. Popescu, “Bell Inequalities for Arbitrarily High-Dimensional Systems,” Phys. Rev. Lett. **88**, no.4, 040404 (2002)
- [32] A. Acin, T. Durt, N. Gisin and J. I. Latorre, “Quantum nonlocality in two three-level systems,” Phys. Rev. A **65**, 052325 (2002) [arXiv:quant-ph/0111143 [quant-ph]].
- [33] G. L. Kane, G. A. Ladinsky and C. P. Yuan, “Using the Top Quark for Testing Standard Model Polarization and CP Predictions,” Phys. Rev. D **45**, 124-141 (1992)
- [34] M. Cepeda, S. Gori, P. Ilten, M. Kado, F. Riva, R. Abdul Khalek, A. Aboubrahim, J. Alimena, S. Alioli and A. Alves, *et al.* CERN Yellow Rep. Monogr. **7**, 221-584 (2019) [arXiv:1902.00134 [hep-ph]].
- [35] ATLAS Collaboration, Trigger menu in 2017, Technical Report No. ATL-DAQ-PUB-2018-002, CERN, Geneva, 2018.
- [36] A. Hayrapetyan *et al.* [CMS], “Measurements of inclusive and differential cross sections for the Higgs boson production and decay to four-leptons in proton-proton collisions at $\sqrt{s} = 13$ TeV,” JHEP **08**, 040 (2023) [arXiv:2305.07532 [hep-ex]].